Japan Architectural Review
Open Access

Architectural Institute of Japan

Translated Paper

Methodology to evaluate the collapse limit state of R/C frames based on the seismic response spectrum

Kazuto Matsukawa[1] and Masaki Maeda[2]

[1]Institute of Industrial Science, The University of Tokyo, Tokyo, Japan; [2]Graduate School of Engineering, Tohoku University, Sendai-shi, Miyagi, Japan

Correspondence
Kazuto Matsukawa, Institute of Industrial Science, The University of Tokyo, Tokyo, Japan.
Email: mtkw@iis.u-tokyo.ac.jp

Funding information
Japan Society for the Promotion of Science, Grant/Award Number: 23360238

The Japanese version of this paper was published in volume 78, number 693, pages 1913-1921, https://doi.org/10.3130/aijs.78.1913 of the *Journal of Structural and Construction Engineering (Transactions of AIJ)*. The authors have obtained permission for secondary publication of the English version in another journal from the Editor of *Journal of Structural and Construction Engineering (Transactions of AIJ)*. This paper is based on the translation of the Japanese version with slight modifications.

Received February 23, 2018; Accepted June 13, 2018

doi: 10.1002/2475-8876.12058

Abstract

This study proposes a method to evaluate the collapse limit displacement of reinforced concrete buildings based on the seismic response spectrum as a more practical alternative to previous methods based on dynamic analysis. The collapse limit displacement estimated by the proposed method is compared to that obtained by dynamic analysis-based methods using artificial and observed ground motions. The results of the proposed method correspond well to the dynamic analysis results. However, models with a natural vibration period of 0.2 s exhibited a large dispersion in the results.

Keywords
capacity deterioration, capacity spectrum method, collapse, safety limit state, shear failure

1. Introduction

In Japanese structural design, the safety limit of building structures, which is defined as the ultimate state of the structure that ensures human safety at the design earthquake load, is commonly considered the first shear failure of a structural member. This definition is used because the capacity deterioration phenomena that occur after shear failure are complex and cannot be precisely modeled. Therefore, the safety limit is often estimated as a conservative value compared to the actual collapse limit which is defined as the ultimate state at which the horizontal and vertical capacity are lost.

Even if shear failure occurs in beams, columns, walls, or other structural members, life safety may be maintained if the surviving ductile members are able to carry horizontal and vertical loads. Therefore, for rational and accountable seismic design, it is preferable to consider capacity deterioration phenomena after shear failure in safety limit estimation.

Incremental dynamic analysis[1] (IDA) is often adopted to estimate the collapse safety of building structures and is a computational method where ground motions are applied to the structure increasingly until a target behavior (shear failure, yielding, collapse, etc.) appears. Maeda and Kang[2] performed IDA for single-degree-of-freedom (SDOF) systems to obtain the ground motion intensity at which the system reaches its ultimate displacement and to quantify the residual capacity of earthquake-damaged building structures. Haselton et al.[3] assessed the collapse risk of structures designed according to the ASCE 7 (ASCE 2002, 2005) and ACI 318 standards using the IDA method. The IDA was applied until the structure collapses, as shown in Figure 1. Haselton et al.[3] defined collapse as the occurrence of dynamic instability during dynamic analysis; therefore, the maximum response against the maximum amplified ground motion in the range where dynamic instability does not occur in the IDA, is considered as the collapse limit displacement, even if the structure is in the capacity deterioration region.

Although the collapse limit and the safety limit which is calculated by multiplying the collapse limit displacement and a rational safety factor may exceed the conventional safety limit (the first shear failure in a static pushover analysis) and may also be in the capacity deterioration region, the IDA-based method is considered more rational than the conventional method because the characteristics of both building structures and ground motions are taken into account. It is obvious that the ground motion characteristics affect the seismic response; therefore, the collapse limit definition which is based on both the building structures and the ground motions as mentioned

above is considered rational, even if the conventional safety limit is set without considering ground motion characteristics.

However, structural engineers who use the IDA method must be knowledgeable and experienced and must know how to perform the time-consuming calculations. Therefore, the IDA-based method is impractical, and a simple alternative method of estimating the collapse limit without nonlinear dynamic analysis is needed.

The authors proposed a method to evaluate the collapse limit of structures using an earthquake response spectrum and the capacity curve of the structure; this method is referred to as the capacity spectrum method (CSM)-based method[4-6] and is considered more practical than the IDA-based method because nonlinear dynamic analyses are not required. The CSM-based method is advantageous in that it includes the effect of the vibration properties of both the structures and ground motions; therefore, the method has high accountability compared to the conventional safety limit assessment in terms of the relation between the ground motion and structural damage. However, in the aforementioned papers,[4-6] the accuracy of the CSM-based method comparing the IDA-based method has not been mentioned. In this paper, further studies to confirm the accuracy of the CSM-based method for SDOF systems were performed by comparing its results with those derived from the IDA-based method.

Prior studies have performed similar research activities, which are summarized here. Kuramoto et al.[7] performed studies to validate the equivalent linearization method through comparing the earthquake response by CSM and dynamic analysis. Inai et al.[8,9] conducted nonlinear dynamic analyses using SDOF systems with and without lateral capacity deterioration to study the effect of asymmetric response behavior in CSM.

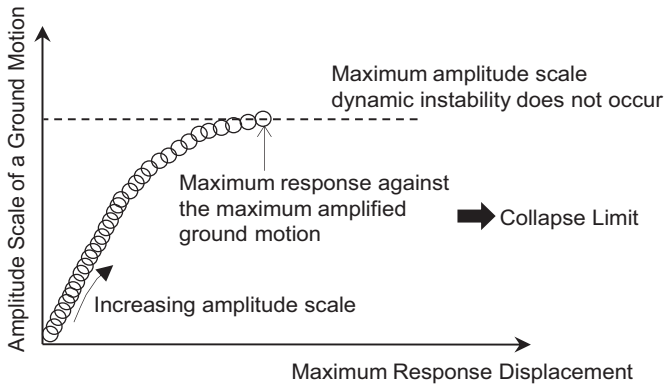

Figure 1. Evaluation of the collapse limit based on IDA

Yoshikawa et al.[10] studied the applicability of the equivalent linearization method and CSM in models consisting of brittle shear members and ductile flexural members. Fujii[11] conducted computational studies for reinforced concrete (RC) frame structures consisting of brittle shear columns and ductile flexural columns using pushover analyses. The results were converted into an equivalent SDOF system to estimate the maximum response using the CSM.

Referring to the studies outlined above, the present paper features CSM application in collapse limit estimation.

2. Methods for calculating the collapse limit using the seismic response spectrum

2.1 Outlines of the calculation

The seismic response of structural systems that retain a stable yield strength (without capacity deterioration), as shown in Figure 2A, is typically evaluated to determine the point of intersection (response point) between the capacity curve of the structural system and the demand spectrum which is multiplied by a damping reduction factor. In this case, the point of intersection can be determined because the idealized capacity curve exhibits stable yield strength and the seismic response spectrum decreases over a large lateral displacement range. However, capacity degradation occurs in real building structures because of brittle failure and shear failure after flexural yielding, even if the structure consists of ductile flexural members. In such cases, a point of intersection will not appear if the response spectrum is considerably larger than the building capacity; in this case, the structure is considered to have collapsed, as shown in Figure 2B.

If the seismic response spectrum decreases such that it gradually becomes closer to the capacity curve until it finally overlaps with the capacity curve, as shown in Figure 3A, then the point of intersection can be determined, and the collapse of the structure is avoided. This point of intersection denotes the maximum response point at which the structure does not collapse for the maximum resistible scaled ground motion and has the same meaning as the collapse limit obtained using the IDA-based method, as shown in Figure 1. Therefore, this point of intersection is considered the collapse limit for CSM-based evaluation.

The procedure for the CSM-based evaluation is as follows.

First, the seismic performance index[12,13] (SPI) for the equivalent SDOF system, which is typically obtained from the nonlinear static analysis (pushover analysis) results, should be calculated for all pushover steps. The SPI is defined as the ratio of the intensity of the capacity earthquake spectrum at each response point to the intensity of the specific standard

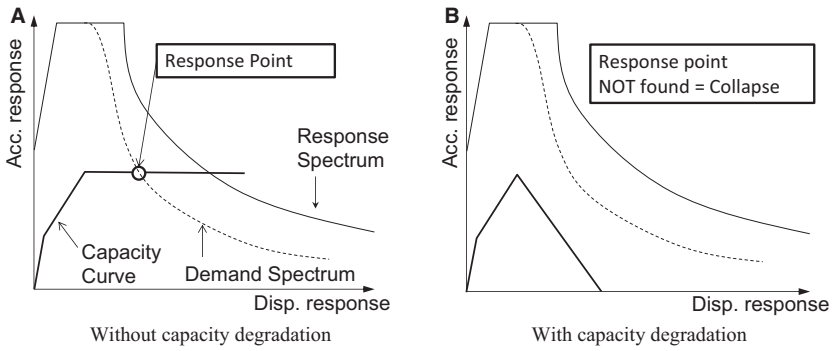

Figure 2. General concept for response estimation with and without capacity degradation

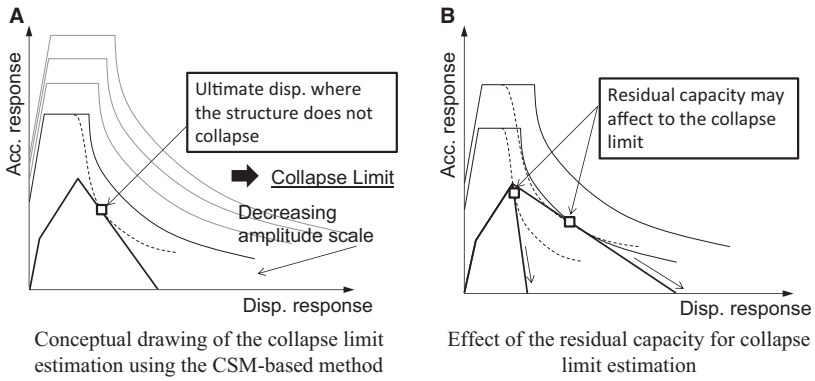

Figure 3. CSM-based collapse limit estimation method

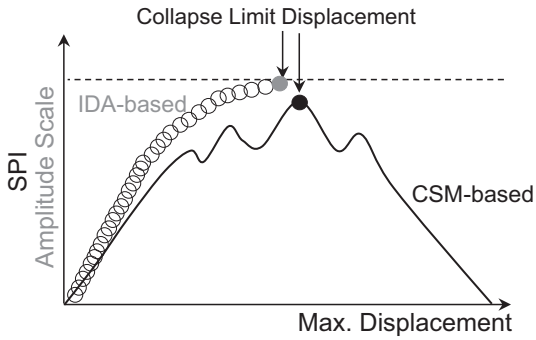

Figure 4. Consistency between collapse limit evaluations using the CSM-based and IDA-based methods

spectrum (5% damping). The capacity spectrum at each step is defined as the 5% damping response spectrum where its demand spectrum intersects the response point on the capacity curve. Therefore, the increments in the SPI will approximately correspond to the amplitude scale of the IDA, as shown in Figure 4. Second, the maximum SPI point is taken as the collapse limit. As shown in Figure 4, even if the SPI and amplitude scale obtained using IDA do not correspond to each other, the collapse limit displacement obtained using the CSM-based method accurately estimates the collapse limit obtained using the IDA-based method because both calculations are affected by the vibration periods of both the structure and ground motion. In addition, the effect of the residual capacity of the structures, which is not considered in conventional structural design and performance evaluation, is included in the CSM-based method, as shown in Figure 3B; therefore, the CSM-based method may enable more rational safety limit estimation.

2.2 Consideration of asymmetric behavior

To conduct the CSM in a large displacement range, it is important to consider the effect of asymmetric behavior, which is the difference between the maximum response in the positive and negative directions and is often observed during dynamic analysis; CSM was originally established by considering nearly symmetric behavior. Asymmetric behavior influences both hysteresis damping and the equivalent vibration period, which are significant parameters for CSM.

In this paper, h_{eq} of a structural system, which is the equivalent damping factor and includes both viscous and hysteresis damping, is calculated as a weighted average of h_{eq} for the structural components according to their potential energy. The viscous damping h_V of each component is calculated according to Equation (1)[14]:

$$h_V = \sqrt{\frac{K_{eq}}{K_0}} \cdot h_0 \tag{1}$$

where K_{eq} is the equivalent (secant) stiffness; K_0 is the elastic stiffness; and h_0 is the initial viscous damping factor, which has a value of 0.05 in this paper.

The hysteresis damping is calculated as the ratio of the potential and hysteretic absorbed energies which are shown in Figure 5 (β is discussed below), and is based on the hysteresis model (in this paper, brittle shear failure and flexure-shear models are adopted, as shown in Figure 5) discussed in chapter 3.

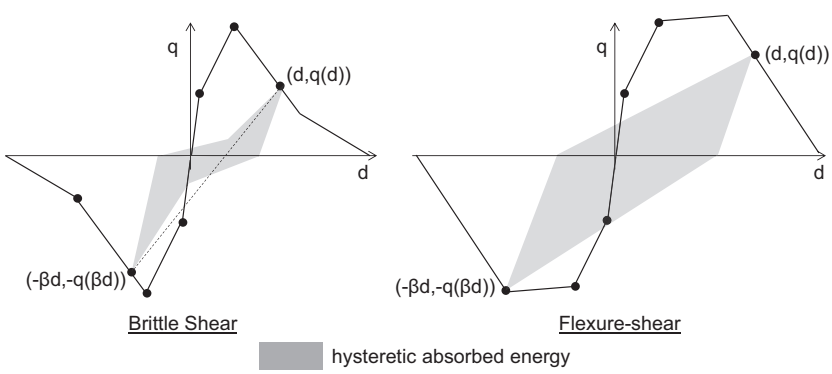

Figure 5. Hysteresis energy absorption model considered in the CSM-based estimation

As noted above and in previous studies,[8,9,15] asymmetric behavior must be considered in hysteresis damping and the equivalent vibration period for accurate evaluation by CSM. Inai et al.[9] proposed a method to evaluate response symmetricity for the capacity degradation model and found that the symmetricity decreases according to the slope of the capacity degradation curve. In this case, a decrease in symmetricity will cause inaccuracies in the hysteresis damping evaluation. In addition, the symmetricity depends on the models and ground motions; therefore, a dynamic analysis must be performed to determine the degree of symmetricity.

The evaluation presented in this paper employs the symmetricity ratio β, which is the ratio of the maximum response in the smaller direction divided by that in the larger direction. β is used to calculate h_{eq} in the calculation of absorbed energy as shown in Figure 5 and is discussed in chapter 3. The potential energy is calculated as the mean of the positive and negative sides.

The equivalent period commonly used in the CSM is calculated based on the equivalent stiffness at the maximum response point even though the equivalent period is significantly shorter. This approach is taken because the CSM typically assumes a steady response and symmetrical behavior. To consider the effect of asymmetric behavior on the vibration period, Okano and Miyamoto[15] proposed an adjustment factor for the equivalent period α_T, which is defined as shown in Equation (2).

$$T'_{eq} = T_{eq}\alpha_T \tag{2}$$

where T_{eq} is the equivalent vibration period based on the equivalent (secant) stiffness in the larger displacement direction and T_{eq}' is the equivalent vibration period based on the equivalent (secant) stiffness derived from a connected line of the maximum response points in both directions. The values of α_T and β are determined based on the dynamic computational analysis discussed in chapter 3. In addition, the relation between α_T and β is shown in Equation (3) based on the assumption of bi-linear backbone curve characteristics.

$$\alpha_T = \sqrt{\beta} \tag{3}$$

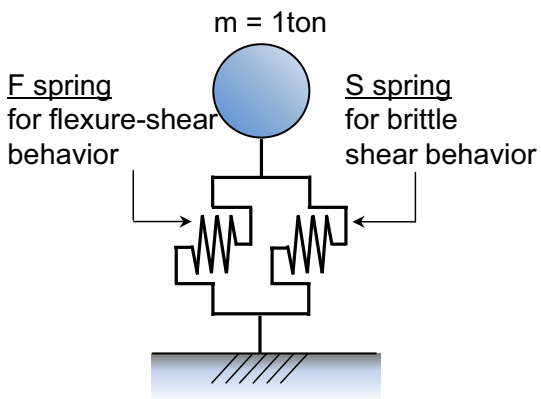

Figure 6. SDOF model used in this paper

3. Studies to discuss the validity of CSM-based collapse limit estimation for the response spectrum described in the Japanese seismic design code

3.1 Computational model

This study employs SDOF systems that have a mass with 2 shear springs in parallel (Figure 6). Backbone characteristics are applied to each shear spring to demonstrate the shear critical member and flexure-shear member. As shown in Figure 6, the spring that acts as the brittle shear member is called the "S spring," and the spring that acts as the flexure-shear member is called the "F spring." The idealized backbone curve of the S spring is determined by referring to the model proposed by Yoshimura[16]

The parameters of the SDOF systems are the initial natural period (T = 0.2, 0.3, 0.4. . .0.8 s), μ_{fu} (see Figure 7, μ_{fu} = 2, 3 and 4) and the maximum strength ratio of the 2 shear springs (S spring (V_{su}) F spring (V_y) = 1:1, 1:2). The sum of V_y and V_{su} is 0.6 of the shear coefficient, however, the calculated maximum shear coefficient of the SDOF system is approximately 0.5 because capacity degradation of S spring starts prior to flexural yielding of F spring. As an example, Table 1 shows the parameters for each spring and the overall system when V_{su}: V_y = 1:1 and Figure 8 shows the backbone curve of the overall system when V_{su}: V_y = 1:1 and μ_{fu} = 3.

The hysteresis behavior proposed by Takeda et al.[17-19] is used in each spring. For the S spring, the Takeda-pinching model is applied to consider the effect of the deterioration of the bonding strength between the steel bars and concrete. For the F spring, pinching is not considered in the hysteresis loop to demonstrate the large energy absorption. The differences in hysteresis characteristics are considered in the calculation of hysteretic energy absorption as shown in Figure 5. In addition, the P-δ effect is not considered in this analysis.

The SDOF system is modeled to demonstrate the dynamic behaviors of both the total collapse mechanism of building structures and the story collapse mechanism (the authors have confirmed that the backbone curves of the SDOF systems are similar to the backbone curve converted from the results of

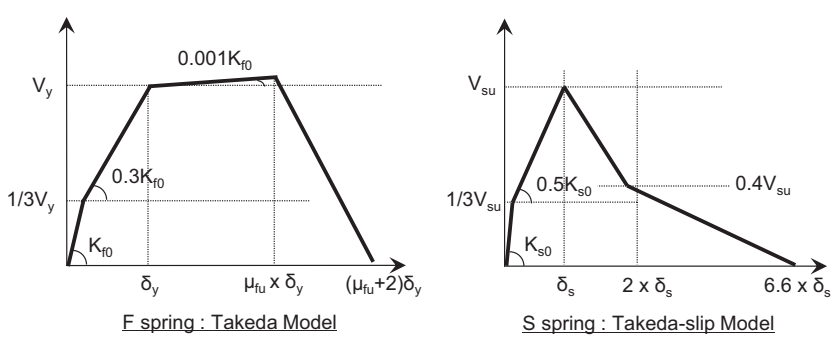

Figure 7. Idealized backbone characteristics of the S spring and F spring

Table 1. Parameters for each spring and the overall system

		0.2 s		0.3 s		0.4 s		0.5 s		0.6 s		0.7 s		0.8 s	
	Unit	S	F	S	F	S	F	S	F	S	F	S	F	S	F
Disp. at 1/3 V_{su} or 1/3 V_y	cm	0.2	0.2	0.4	0.4	0.7	0.7	1.1	1.1	1.6	1.6	2.2	2.2	2.9	2.9
1/3 V_{su}/weight or 1/3 V_y/weight	-	0.09	0.09	0.09	0.09	0.09	0.09	0.09	0.09	0.09	0.09	0.09	0.09	0.09	0.09
δ_s or δ_y	cm	1.0	1.6	2.3	3.5	4.1	6.3	6.3	9.8	9.1	14.1	12.4	19.2	16.2	25.1
V_{su}/weight or V_y/weight	-	0.30	0.30	0.30	0.30	0.30	0.30	0.30	0.30	0.30	0.30	0.30	0.30	0.30	0.30
Max. capacity of system	-	0.51		0.51		0.51		0.51		0.51		0.51		0.51	
$\mu_{fu}\times\delta_y$: (μ_{fu} = 2)	cm	-	3.1	-	7.1	-	12.6	-	19.6	-	28.3	-	38.5	-	50.3
$\mu_{fu}\times\delta_y$: (μ_{fu} = 3)	cm	-	4.7	-	10.6	-	18.8	-	29.4	-	42.4	-	57.7	-	75.4
$\mu_{fu}\times\delta_y$: (μ_{fu} = 4)	cm	-	6.3	-	14.1	-	25.1	-	39.3	-	56.5	-	77.0	-	100.5
(μ_{fu}+2)δ_y: (μ_{fu} = 3)	cm	6.8	7.9	15.2	17.7	27.0	31.4	42.2	49.1	60.8	70.7	82.8	96.2	108.1	125.6
Disp at capacity of system = 0: (μ_{fu} = 3)	cm	7.9		17.7		31.4		49.1		70.7		96.2		125.6	

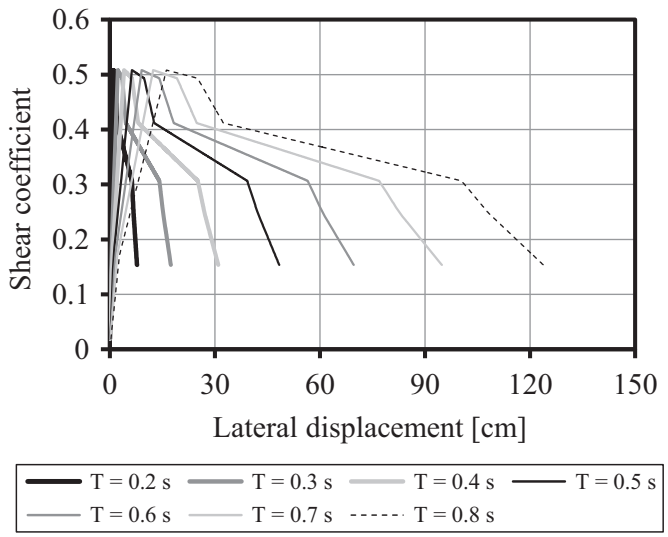

Figure 8. Backbone characteristics for the SDOF system (μ_{fu} = 3)

nonlinear static analysis for the story collapse mechanism which was obtained in a previous study[20]). Although Figure 9 shows a conceptual example of the total collapse mechanism as a target type of the structure, the SDOF model in this study is assumed to employ a greater number of brittle shear members than that of the example, referring to the models for V_{su}: V_y = 0.5:1 or 1:1. It is often difficult to estimate the earthquake response using the CSM for structures mainly comprising brittle shear members because of the large asymmetric behavior. In this study, this negative and difficult model structure is employed to consider adverse conditions to validate the CSM-based collapse limit estimation.

3.2 Ground motions

A set of ground motions consisting of ten artificial ground motions was used to fit the response spectrum provided in the Japanese building code (soil type 2). The 5 artificial ground motions with a duration of 30 s (principal motion duration = 10 s) are called the S series, and the other 5 ground motions with durations of 120 s (principal motion duration = 60 s) are called the LL series. Each ground motion is denoted by a combination of the series name and identification number, such as "LL05" or "S03". The time-histories of the S01 and LL01 waves are shown in Figure 10. The response spectrum calculated using the artificial ground motions and target spectrum is shown in Figure 11. The spectra exhibit good agreement with each other.

3.3 Collapse limit obtained using the IDA method

3.3.1 Analytical method

In this section, as shown in Figure 1, the increasingly scaled artificial ground motions are applied to the SDOF system

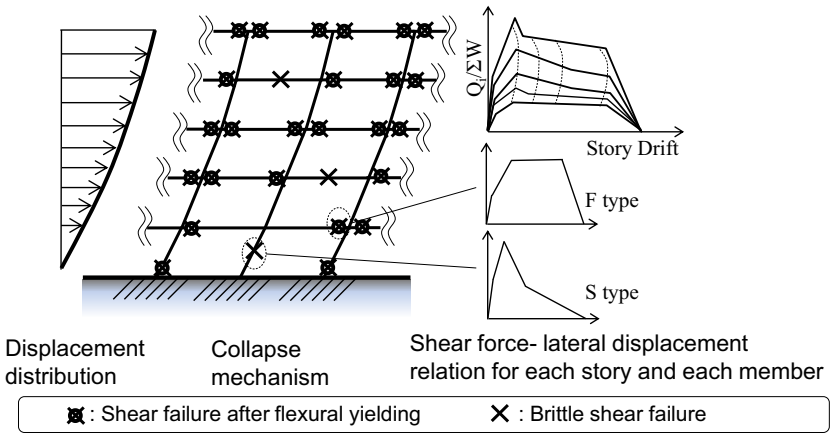

Figure 9. Conceptual drawing of the total collapse mechanism of building structures considered in this study

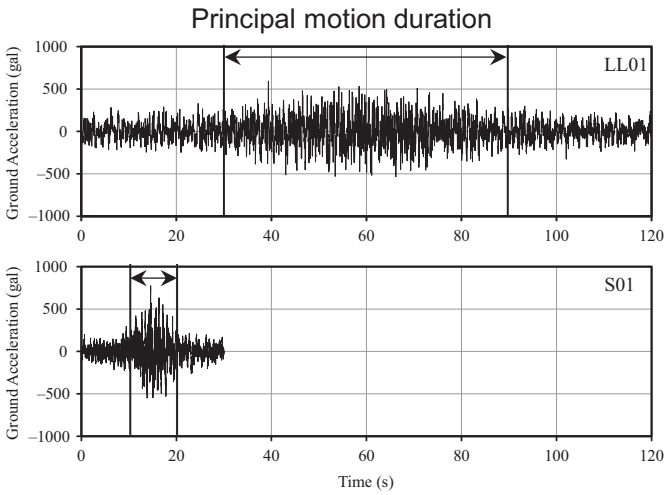

Figure 10. Time-history of artificial ground motion, LL01 wave (top) and S01 wave (bottom)

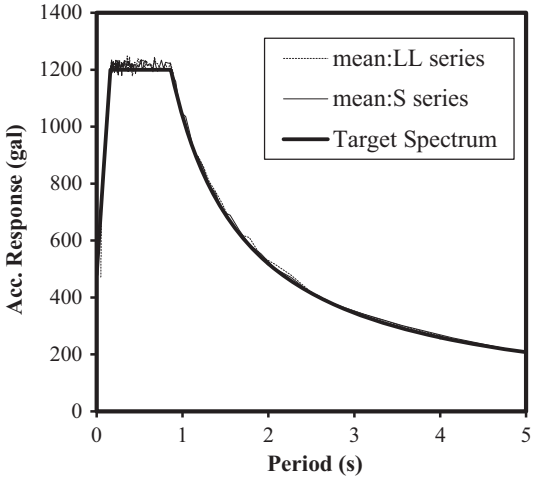

Figure 11. Averaged spectral acceleration of both series of artificial ground motions

models in ascending order until collapse occurs. The ultimate lateral displacement of the maximum-scaled ground motion at which dynamic instability does not occur is considered the collapse limit displacement by the IDA-based method. The Newmark-β method is used for the computations, and the unbalanced force is carried over to the next computational step and canceled. Viscous damping is assumed to be 5% of the tangent stiffness of each spring in each step if the spring has a positive tangent stiffness. If the tangent stiffness is negative in capacity degradation regions, zero damping is assumed. Several previous studies have used different assumptions than this study; for example, Yoshimura[21] assumed constant viscous damping and a linear relationship for positive initial stiffness. However, other previous studies[22] have employed the same assumptions as this paper.

The ground motion amplitude increased from 0.01 by 0.05; the authors confirmed that there was an approximately 10% change in the collapse limit displacement when using different increments from 0.001 to 0.1.

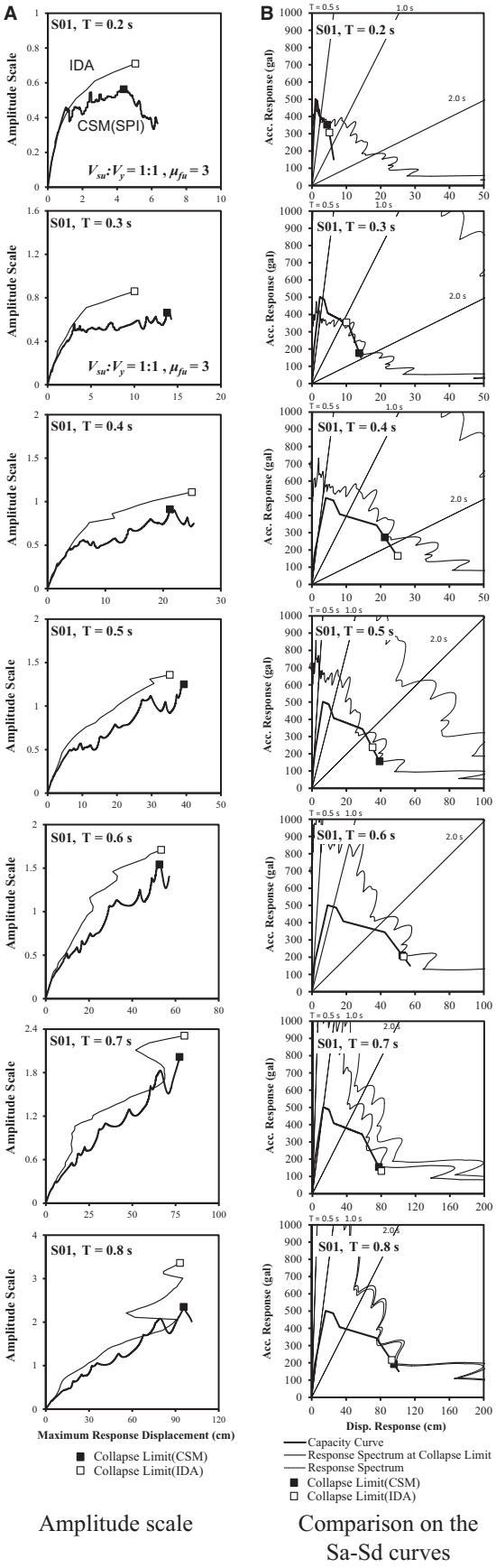

Figure 12. Analytical results against artificial ground motions (V_{su}: V_y = 1:1, μ_{fu} = 3)

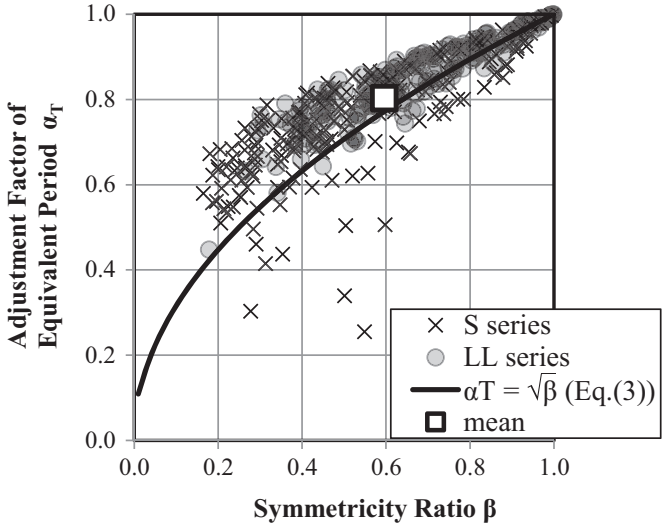

Figure 13. α_T vs β at the collapse limit calculated using the IDA-based method

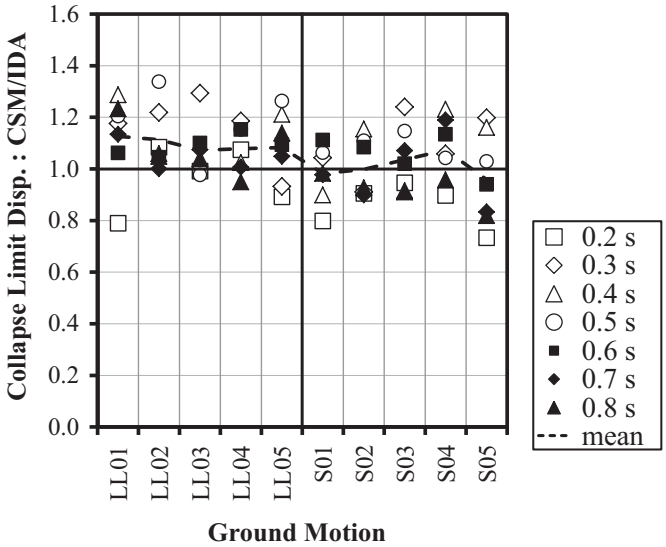

Figure 14. Accuracy of the collapse limit evaluation for artificial ground motions

3.3.2 Results

Example IDA results are shown by the sharp line in Figure 12A, which represents V_{su}: V_y = 1:1 and μ_{fu} = 3 against the S01 wave. Figure 12B shows the collapse limit estimation results plotted on the capacity curve of the models. The outlined box plot in Figure 12A and B denotes the collapse limit estimated by the IDA-based method. The maximum response increases according to amplitude of ground motion, and the collapse limits are estimated to be less than 60% of the maximum capacity of the structure.

3.3.3 Relation between α and β

The α_T and β values at the collapse limit, which will be used in the CSM-based method, are calculated from the results derived from the IDA-based method using artificial waves. Figure 13 shows the calculated values of α_T and β at the collapse limit. The black line is derived from Equation (3) and is highly similar to the computational results. The results illustrate that the S series waves exhibit less symmetricity than the LL series waves.

The average values for α_T and β are 0.80 and 0.60, respectively, and these values are used in the CSM calculations. These values are consistent with a previous study that obtained a value of α_T = 0.82.[15]

3.4 Accuracy of the CSM-based method

Figure 12A and B show the results of the collapse limit evaluation of both methods with the collapse limit point on the capacity curve of the structures. The collapse limit points obtained using both methods are in good agreement. In addition, SPI calculations were performed until the strength of the model deteriorated by 30% of the maximum strength of the system by considering the application range.

The collapse limit displacement calculated by the CSM-based method was divided by the collapse limit displacement calculated by the IDA-based method, and the results are plotted along the vertical axis of Figure 14. The results are averaged and arranged by each ground motion and initial vibration period T of each structural system. The collapse limit displacement in Figure 14 demonstrates the validity of the CSM-based evaluation. The errors are within approximately ±20%. Regarding the effect of the duration of the ground motion, the collapse limit displacements for the S series ground motions are more accurate than those of the LL series ground motions, which are

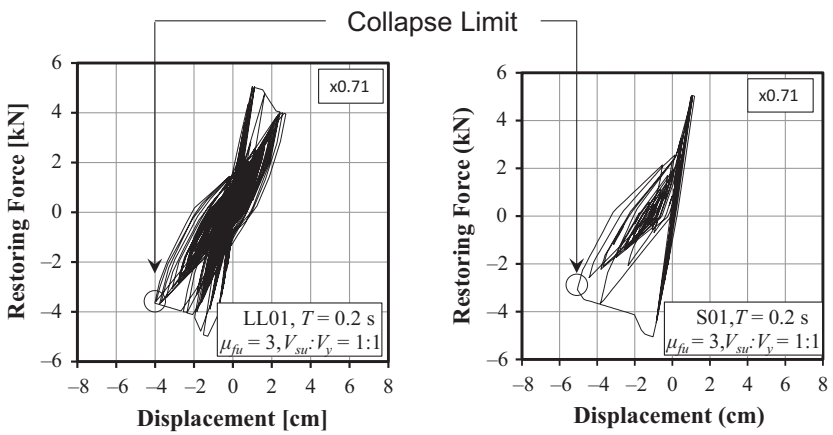

Figure 15. Results of the dynamic analysis for the LL01 wave (left) and S01 wave (right)

overestimated by 10% on average. Figure 15 shows 2 dynamic analysis examples for the $T = 0.2$ s and V_{su}:V_y = 1:1 model; the S01 and LL01 waves with scaling to reach the collapse limit are used as inputs. Figure 15 illustrates that the LL01 wave exhibits a more symmetrical response than the S01 wave; therefore, the maximum response (collapse limit) against the S01 wave is larger. Such dynamic behavior has been observed previously.[23] This behavior affects the IDA-based results and may be responsible for the 10% overestimation noted above.

The effect of the vibration period T can be found from Figure 14. The structural system with a short natural period (eg, $T = 0.2$ s or 0.3 s, denoted by the open symbols in Figure 14) exhibits large variability. This trend occurs because the increment in the SPI near the collapse limit for the models with a shorter T is slower as shown in Figure 12A and both the response spectrum and capacity curve show a similar degradation slope, as shown in Figure 12B. If the SPI increment is slower because of the similar slope, a slight roughness in the response spectrum generates an unevenness in the SPI and variability in the estimated collapse limit displacement.

Figure 16 shows the amplitude of the input ground motion at the collapse limit. The amplitude scale calculated by the CSM-based method is underestimated relative to that obtained using the IDA-based method.

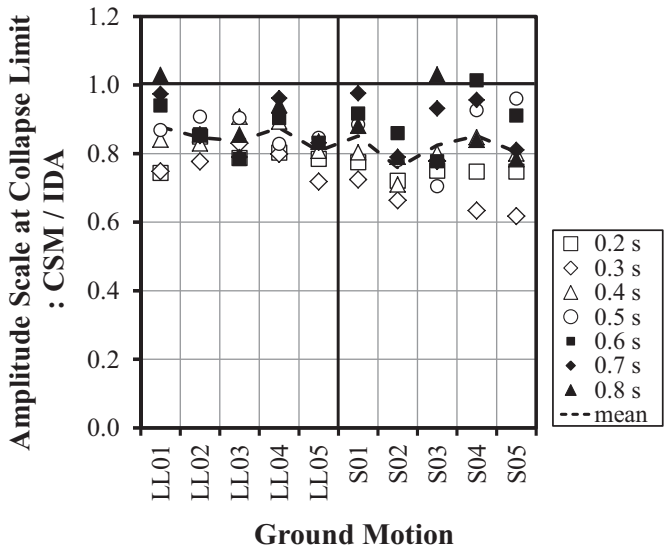

Figure 16. Accuracy of the amplitude scale at the collapse limit for artificial ground motions

3.5 Validity of hysteresis damping

The substitute viscous damping,[24,25] which is described in Equation (4), was calculated using the dynamic analysis results above to validate the equivalent damping factor h_{eq} defined in Section 2.2.

$$h_S = -\int_0^t \ddot{y}_0 \dot{y} dt \Big/ \left(2\omega \int_0^t \dot{y}^2 dt\right) \tag{4}$$

where $\ddot{y}_0$ and $\dot{y}$ are the ground acceleration and response velocity, respectively, and ω is the angular frequency, which is calculated as the secant stiffness between the maximum negative and positive responses. The results for $h_{eq,s}$ and $h_{eq,f}$ (the equivalent damping factors for the S and F springs, respectively), and for h_{eq} and h_s for a model with $T = 0.4$ s, V_{su}:V_y = 1:1, and $\mu_{fu} = 4$, against the S01 and LL01 waves are shown in Figure 17 with the backbone curve of each spring and the overall model. The value of h_s is underestimated when using h_{eq} in the CSM-based method; therefore, the amplitude scale discussed in Section 3.4 is also underestimated. However, the trends of the increments for both h_{eqs} and h_s are similar according to the maximum response displacement.

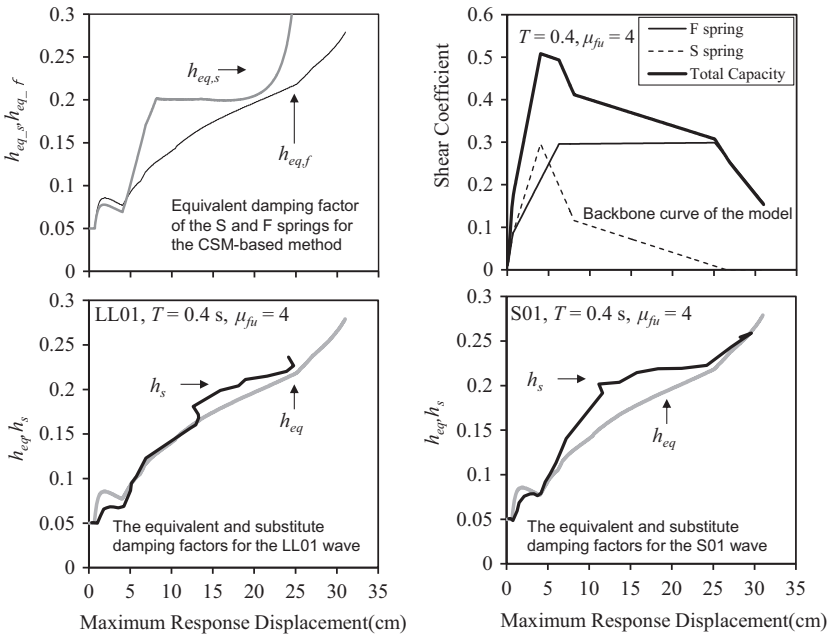

Figure 17. Equivalent damping factor of the S and F springs for the CSM-based method (top left), backbone curve of the model (top right), and comparisons between the equivalent and substitute damping factors of the LL01 wave (bottom left) and S01 wave (bottom right)

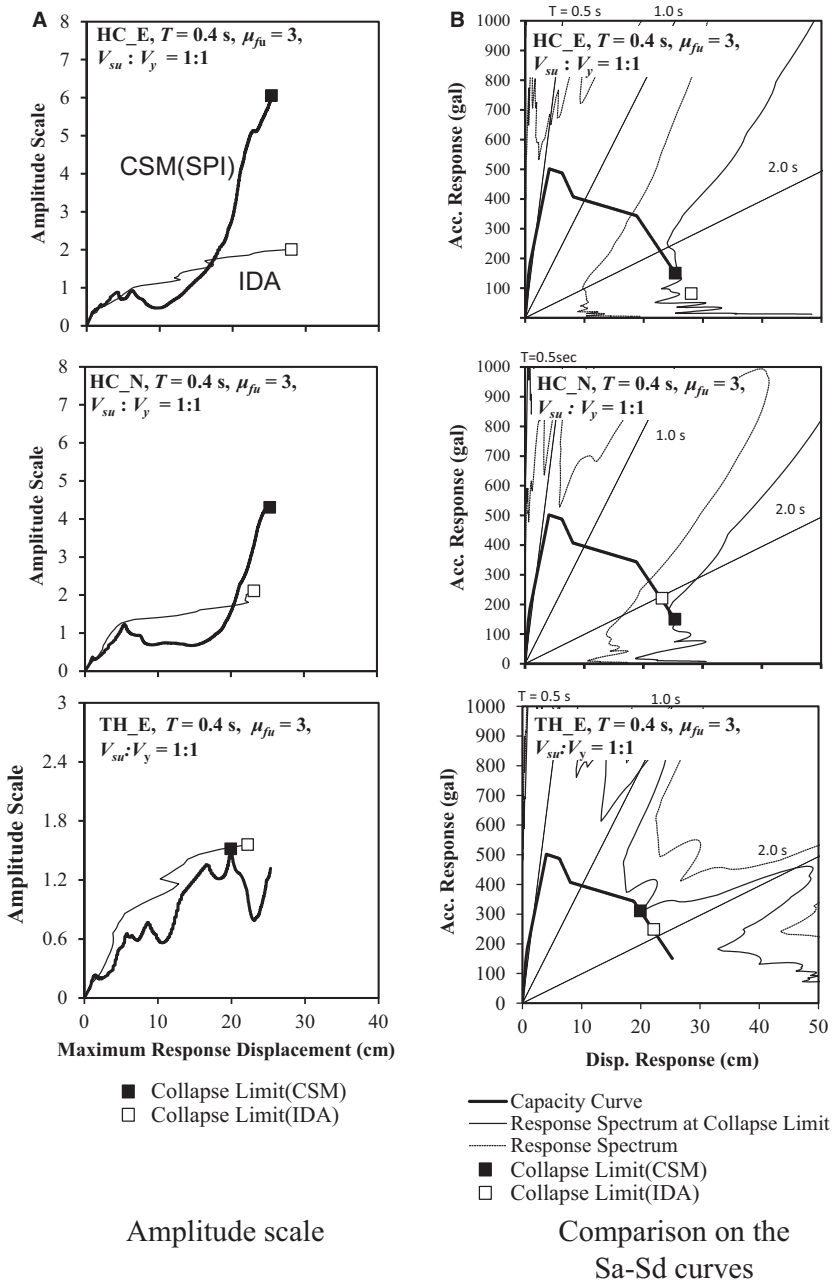

Figure 18. Analytical results for the observed ground motions (high accuracy example)

4. Studies against observed ground motions

4.1 Ground motions

The ground motions used in this chapter consist of twelve ground motions observed at 6 stations including both the NS (N) and EW (E) directions; the El Centro wave (1940, EL_N and EL_E); Kobe wave (1995, KB_N and KB_E); Hachinohe wave (1968, HC_N and HC_E); Ojiya wave (2004, OJ_N and OJ_E); Taft wave (1952, TF_N and TF_E); and Tohoku wave (1978, TH_N and TH_E). The acceleration records are amplified such that the response spectrum velocity corresponds to 165 kine.

4.2 Analytical results

Examples of the HC_E, HC_N and TF_E waves for T = 0.4 s, V_{su}:V_y = 1:1, and μ_{fu} = 3 are shown in Figure 18A and B, and the relationships between the SPI and amplitude scale are shown in Figure 18B as examples of relatively corresponding results. Figure 18A and B illustrate that the collapse limits obtained using the CSM- and IDA-based methods correspond in ranges where the response spectrum has a convex shape toward the origin. The SPI is significantly greater in those ranges because of the convex shape of the response spectrum and because of plasticity (damping); thus, the SPI peaks were clarified. Therefore, it is possible to obtain accurate and reliable results using the CSM-based method for such ground motions. By contrast, the results shown in Figure 19A and B, which are for T = 0.3 s, μ_{fu} = 4, and V_{su}:V_y = 0.5:1 for the TH_N wave, are an example where the results do not correspond to each other. The results exhibit several SPI peaks, and the difference between each SPI peak is relatively small; therefore, such differences affect the accuracy of the collapse limit estimation.

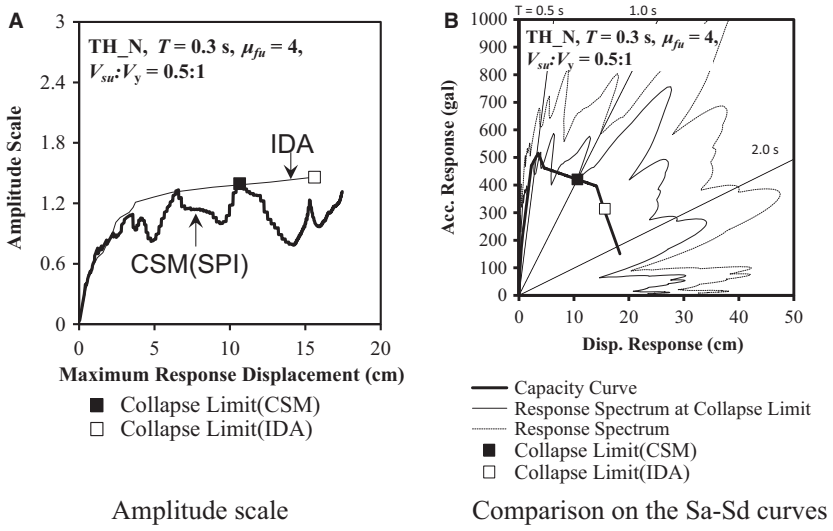

Amplitude scale Comparison on the Sa-Sd curves

Figure 19. Analytical results for the observed ground motions (low accuracy examples)

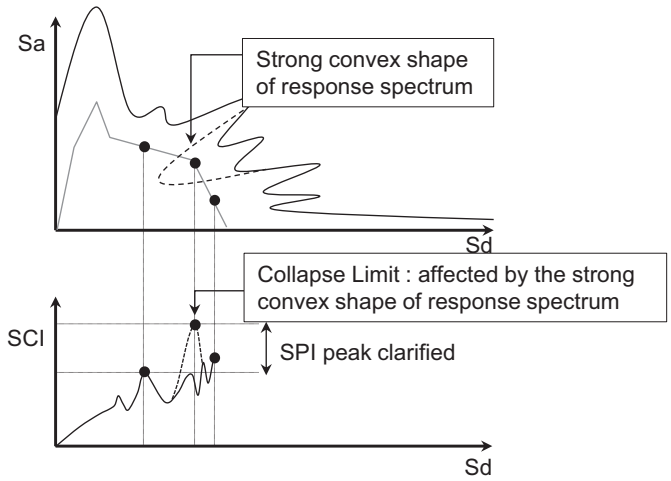

Figure 20. Convex shape of the spectrum and its influence

If a large convex shape is observed in the response spectrum, the SPI peak will be clear, and such periodic effects may affect the dynamic analysis. Figure 20 shows a conceptual drawing of this situation and illustrates that the CSM-based method is suitable for ground motions that have strong periodical deference.

Figure 21A and B show the accuracy of the collapse limit displacement, and Figure 22A and B show the amplitude at the collapse limit. Figures 21A and 22A include all results, whereas Figures 21B and 22B exclude the results for the $T = 0.2$ models. The accuracy of the collapse limit displacement obtained with the CSM-based method varies considerably more when including the $T = 0.2$ models than when the $T = 0.2$ models are excluded. The standard deviation decreases from 0.30 to 0.19 if the results for the $T = 0.2$ models are omitted, as shown in Figure 21B. As noted in Chapter 3, the cases with $T = 0.2$ (or models with shorter natural periods) have considerable scattering because of their capacity degradation slope.

The amplitude scale at the collapse limit, as shown in Figure 22B, widely varies even if the results with longer values of T are included. This result suggests that although the convex shape of the response spectrum may aid the evaluation of the collapse limit displacement in terms of clarifying the SPI peak, the shape is responsible for the difference in amplitude scale between the IDA- and CSM-based methods.

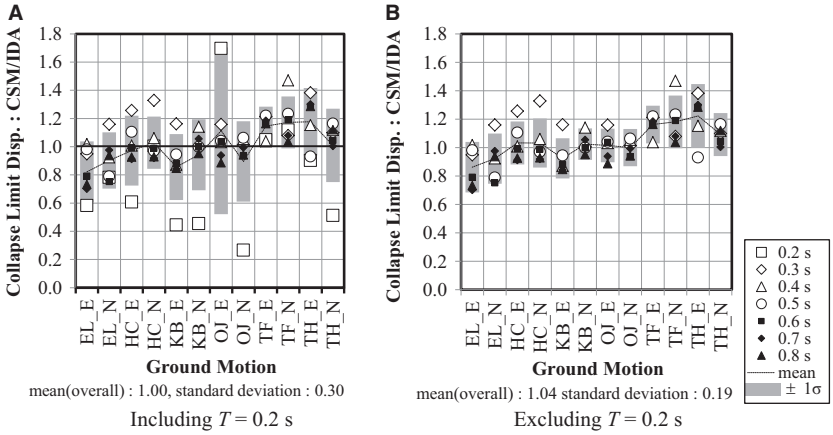

Including $T = 0.2$ s Excluding $T = 0.2$ s

Figure 21. Accuracy of the collapse limit evaluation for the observed ground motions

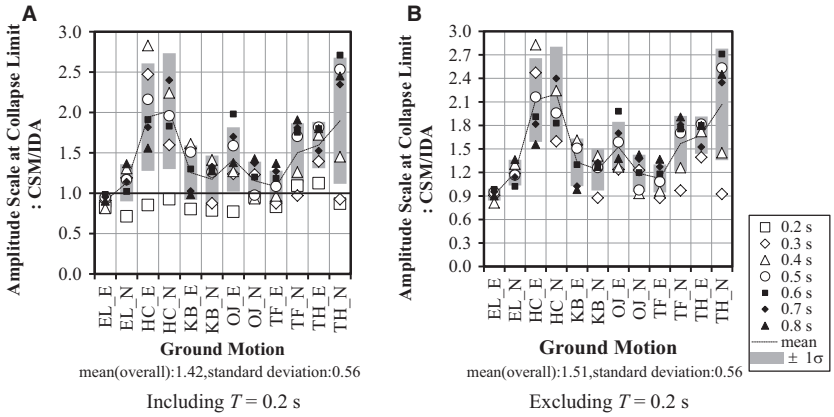

Including $T = 0.2$ s Excluding $T = 0.2$ s

Figure 22. Accuracy of the amplitude scale at the collapse limit for the observed ground motions

The CSM-based method is suitable for evaluating the collapse limit displacement, even if observed ground motions are used, except for structural systems with a short vibration period.

5. Conclusions

1 This study proposed a CSM-based method as a practical alternative to the IDA-based method for evaluating the collapse limit of structures.
2 The equivalent period α_T and symmetry ratio β are adjusted to evaluate the asymmetric behavior in the CSM-based method. The values of α_T and β are obtained from a dynamic analysis, and h_{eq} is calculated considering the asymmetric behavior, and exhibits good agreement with h_s (substitute viscous damping, which is calculated from the dynamic analysis).
3 The collapse limit displacement obtained using the CSM-based method corresponds well with that obtained using the IDA-based method except for structural systems with short natural periods.
4 Ground motions with durations of 30 and 120 s were used. The differences in the duration time changed the collapse limit displacement by 10%.
5 The convex shape in the response spectrum significantly affected the accuracy of the CSM-based method. Ground motions with large convex shapes exhibited higher accuracy.

Acknowledgment

This work was supported by JSPS KAKENHI grant number 23360238.

Disclosure

The authors have no conflict of interest to declare.

References

1 Vamvatsikos D, Allin Cornell C. Incremental dynamic analysis, *Earthquake Engineering and Structural Dynamics*, pp. 491-514, Volume 31, Issue 3, 2002.
2 Maeda M, Kang DE. Post-earthquake damage evaluation of reinforced concrete buildings, *Journal of Advanced Concrete Technology*, Vol. 7, No.3, Japan Concrete Institute, pp.327-335, 2009.
3 Haselton CB, Liel AB, Deierlein GG, Dean BS, Chou JH. Seismic collapse safety of reinforced concrete buildings. I: Assessment of ductile moment frames, *Journal of Structural Engineering, ASCE*, pp. 481-491, 2011.
4 Matsukawa K, Miura K, Maeda M. Sendanhakai suru hasira de kousei sareru tekkinnkonkuri-tozou honegumi no anzengenkai hyoukahou ni kansuru kenkyu (Collapse Limit Evaluation of Reinforced Concrete Frame Structure composed of Shear Column), *Proceedings of the Japan Concrete Institute*, Vol.33, No.2, pp.31-36, 2011. (In Japanese).
5 Matsukawa K, Maeda M, Miura K, Takahashi K. Evaluation of deformation capacity at collapse of R/C frame composed of shear and flexural columns. *Kozo Kogaku Ronbunshu (Journal of Structural Engineering)*, Vol. 58B., pp. 25-32, 2012. (In Japanese).
6 Matsukawa K, Maeda M, Al-Washali H, Takahashi K. Research for collapse of R/C frame composed of shear and flexure column, *Proceedings of the 15th WCEE*, paper No. 1501, 2012.
7 Kuramoto H, Teshigawara M, Okuzono T, Koshika N, Takayama M, Hori T. Predicting the earthquake response of building using equivalent single degree of freedom system, *Proceedings of the 12th WCEE*, paper No.1039, 2000.
8 Inai E, Kitamura K, Maruhashi N, Hiraishi H. Study on earthquake response and equivalent linearization method of reinforced concrete buildings, *Journal of Structural and Construction Engineering (Transactions of AIJ)*, Vo.75, No.650, pp.859-868, 2010. (In Japanese).
9 Kohara Y, Inai E, Maruhashi N. Study on prediction of earthquake response of reinforced concrete buildings with degrading lateral load carrying capacity, *The Proceedings of the AIJ Annual Conference*, pp.707-708, 2010. (In Japanese).
10 Yoshikawa K, Okano H, Koshika N. Prediction of earthquake response of story shear model which contains brittle elements by equivalent linearization method, *Journal of Structural and Construction Engineering (Transactions of AIJ)*, No.603, pp.47-54, 2006. (In Japanese).
11 Fujii K. Sendanhakai suru buzai wo fukumu kizontekkinkonkuri-tozou tatemono no zisinzisaidaioutou no suitei (Seismic response estimation for existing reinforced concrete buildings containing shear members), *Proceedings of the Japan Concrete Institute*, Vol.32, No.2, pp.787-792, 2010. (In Japanese).
12 Architectural Institute of Japan. Guidelines for Performance Evaluation of Earthquake Resistant Reinforced Concrete Buildings (Draft). Architectural Institute of Japan, 2004. (In Japanese).
13 Kabeyasawa T. An outline of AIJ guidelines for performance evaluation of earthquake resistant reinforced concrete buildings, *Performance-based Seismic Design Concepts and Implementation Proceedings of the International Workshop*, pp.27-38, 2004.
14 Yoshikawa K, Okano H, Koshika N. Evaluation of earthquake response of single-story unsymmentric buildings by equivalent linearization method considering higher mode, *Journal of Structural and Construction Engineering (Transactions of AIJ)*, No.621, pp.57-65, 2007. (In Japanese).
15 Okano H, Miyamoto Y. Equations derived from equivalent linearization method. Consideration based on energy balance and its application to evaluation of probability of excess of deformation capacity, *Journal of Structural and Construction Engineering (Transactions of AIJ)*(In Japanese), No.562, pp.45-52, 2012. (In Japanese).
16 Yoshimura M. Formulation of post-peak behavior of old reinforced concrete columns until collapse, *Proceedings of the 14th WCEE*, Paper ID: 05-03-0104, 2008.
17 Eto H, Takeda T. tekkinkonkuri-to kouzoubutu no dansosei zisin outou fremu kaiseki (Inelastic Seismic Response Analysis for Reinforced Concrete Frame Structures), *The Proceedings of the AIJ Annual Conference*, pp.1877-1878, 1978. (In Japanese).

18 Takeda T, Sozen MA, Nielsen NN. Reinforced concrete response to simulate earthquakes, *Journal of Structural Division, ASCE*, Vol.96, No. ST12, pp.2557-2573, 1970.
19 Kabeyasawa T, Shiohara H, Otani S, Aoyama H. Analysis of the full-scale seven-story reinforced concrete test structure, *Journal(B), The Faculty of Engineering, University of Tokyo*, Vol.XXXVII, No.2, pp. 432-478, 1983.
20 Matsukawa K, Maeda M. Evaluation of collapse deformation for RC frame including lateral strength degradation in members – analysis on frames with story collapse mechanism, *The Proceedings of the AIJ Annual Conference*, pp.627-628, 2012. (In Japanese).
21 Yoshimura M. Nonlinear analysis of a reinforced concrete building with a soft first story collapsed by the 1995 Hyogoken-Nanbu earthquake, *Cement and Concrete Composites*, Volume 19, Issue 3, pp. 213-221, 1997.
22 Nakagawa T. (Daizisinzi ni okeru mokuzou zikugumi kouhou zyuutaku no toukai kaiseki syuhou no kaihatu) Development for collapse analysis method of wooden frame residential building against huge earthquake, *Kenken Research Document*, No.128, Building Research Institute of Japan, p.7, 2010. (In Japanese).
23 Nakamura Y, Kabeyazawa T. Expectation of time-history displacement responses based on characteristics of earthquake motion, *Journal of Structural and Construction Engineering (Transactions of AIJ)*(In Japanese), No.532, pp.51-56, 2000. (In Japanese).
24 Shibata A. Dynamic Analysis of Earthquake Resistant Structure, Tohoku University, 2010.4.
25 Miyashita T, Kuramoto H. A study on evaluation for equivalent damping factor in the calculation of response and limit strength, *The Proceedings of the AIJ Annual Conference*, pp.367-368, 2003. (In Japanese).

How to cite this article: Matsukawa K, Maeda M. Methodology to evaluate the collapse limit state of R/C frames based on the seismic response spectrum. *Jpn Archit Rev*. 2018;00:1–12. https://doi.org/10.1002/2475-8876.12058